Monthly Notices
of the
ROYAL ASTRONOMICAL SOCIETY

MNRAS **492,** 283–293 (2020)
Advance Access publication 2019 December 11

doi:10.1093/mnras/stz3323

Quantifying acetaldehyde in astronomical ices and laboratory analogues: IR spectra, intensities, ^{13}C shifts, and radiation chemistry

Reggie L. Hudson[1]★ and Robert F. Ferrante[2]

[1]*Astrochemistry Laboratory, NASA Goddard Space Flight Center, Greenbelt, MD 20771, USA*
[2]*Chemistry Department, US Naval Academy, Annapolis, MD 21402, USA*

Accepted 2019 November 21. Received 2019 November 19; in original form 2019 October 8

ABSTRACT

Acetaldehyde is of interest to astrochemists for its relevance to both interstellar and cometary chemistry, but little infrared (IR) spectral data have been published for the solid phases of this compound. Here we present IR spectra of three forms of solid acetaldehyde, with spectra for one form being published for the first time. Direct measurements of band strengths and absorption coefficients also are reported for the first time for amorphous aldehyde, the form of greatest interest for astrochemical work. An acetaldehyde band strength at ∼1350 cm^{-1} that has been used as a reference for about 20 yr is seen to be in error by about 80 per cent when compared to the direct measurements presented here. Spectra and peak positions also are presented for H^{13}C(O)^{13}CH$_3$, and then used for the first identification of ketene as a radiation product of solid acetaldehyde.

Key words: astrochemistry – ISM: molecules.

1 INTRODUCTION

The characterization of icy solids continues to interest astrochemists and to require laboratory measurements on a variety of compounds, both organic and inorganic. We recently have explored a number of compounds in order to better quantify infrared (IR) spectral data of known and suspected interstellar and cometary ices. Inorganics examined include CO_2 and N_2O, and organics include ethanol, acetone, and methyl propionate for the alcohol, ketone, and ester classes, respectively.

Of the common families of organic compounds, there are no direct measurements of IR band strengths for any of the known interstellar aldehydes in the solid state, although aldehydes are well established as both interstellar and cometary molecules. In the case of comets, acetaldehyde, HC(O)CH$_3$, was first identified in Comet Hale-Bopp by radio-wave observations (Crovisier et al. 2004), having already been found in the interstellar medium, again at radio wavelengths (Fourikis et al. 1974). Other extraterrestrial aldehydes include the larger molecule propionaldehyde (propanal), HC(O)CH$_2$CH$_3$, and the special case of formaldehyde, H_2CO (Snyder et al. 1969; Hollis et al. 2004). These were detected in the gas phase as opposed to a solid phase, an ice, in part because the solid-phase IR aldehyde absorptions that might be observed tend to overlap with those of more abundant molecules. Nevertheless, astrochemists have long maintained an interest in aldehydes as such molecules can, among other things, be precursors to amino acids via the Strecker synthesis. See, for example, the work of Fresneau et al. (2015) for solid-phase laboratory results related to alanine formation from acetaldehyde.

A different aspect of acetaldehyde astrochemistry, namely the molecule's production, was addressed in a recent paper here on 'The (impossible?) formation of acetaldehyde . . . ' on interstellar grains (Enrique-Romero et al. 2016). The authors' calculations led them to conclude that acetaldehyde cannot be made by the $\dot{C}H_3 + H\dot{C}O$ radical–radical reaction on an interstellar grain if amorphous H_2O-ice is present, although a subsequent computational paper appears to soften this claim (Enrique-Romero et al. 2019). The same authors also pointed out that no H_2O-ice was present in two previous experiments that produced acetaldehyde by electron-radiolysis at 10 K (Bennett et al. 2005) or UV-photolysis at 20 K (Öberg et al. 2009). However, two other reports of acetaldehyde production in H_2O-rich ices at ∼20 K seem to have been missed (Moore & Hudson 1998; Öberg et al. 2010), suggesting a need for further experiments to make this molecule or to verify its formation. Preferably, those experiments should quantify any such formation, or at least place upper limits on acetaldehyde yields.

This latter point is related to a difficult challenge in studying solid-phase aldehydes, and other molecules, the conversion of an IR spectral intensity into a molecular abundance. This typically involves integration of an IR band of interest followed by division of the result by an IR band strength, and thus requires that reference band strengths be available either directly from laboratory measurements or from some type of computational method. One of our group's early contributions to this effort was the measurement of an acetaldehyde IR band strength near 20 K (Moore & Hudson 1998), a result obtained from the linear part of a calibration curve (absorbance versus ice thickness) with the spectrometer

★ E-mail: reggie.hudson@nasa.gov

configured for transflection operation (i.e. transmission–reflection–transmission, TRT, or reflection–absorption–infrared, RAIR). The apparent band strength (A') reported was A'(1350 cm^{-1}, ~7.41 μm) = 6.1 × 10^{-18} cm molecule^{-1}. A difficulty with this A' was that it was calculated using room-temperature liquid-phase values of acetaldehyde's density and refractive index (670 nm), for lack of better supporting data. A greater problem was that this result was obtained from a reflection measurement and not a transmission one. Maeda & Schatz (1961), among others, have noted that IR absorbance can vary non-linearly with ice thickness in reflection measurements, meaning that our A' might not be applicable to other laboratory systems, much less astronomical observations. Its use by, for example, Öberg et al. (2009) could be problematic.

At roughly the same time as our paper appeared, Schutte et al. (1999) published A'(1350 cm^{-1}, ~7.41 μm) = 1.5 × 10^{-18} cm molecule^{-1} for the same acetaldehyde feature. This value has been cited in several subsequent papers, such as Gibb et al. (2004), Dartois (2005), and Vinogradoff et al. (2012), but its heritage is suspect. Schutte et al. (1999) cited a review article (Wexler 1967), but that paper does not mention acetaldehyde or any other aldehyde. A misreading of the latter publication appears to be the source of the error. Still later, Terwisscha van Scheltinga et al. (2018) published an extensive set of acetaldehyde IR spectra, and the suspect A' value of Schutte et al. (1999) was the only acetaldehyde band strength given. Adding to the uncertainty with all of these laboratory results is the value A'(1494 cm^{-1}) = 3.9 × 10^{-18} cm molecule^{-1} for acetaldehyde used by Fresneau et al. (2015). This seems to be from a misreading of a paper on formaldehyde, since acetaldehyde has no IR band at 1494 cm^{-1}.

Faced with these conflicting A' values, Bennett et al. (2005) adopted a different approach, using density-functional theory (DFT) to calculate band strengths for gas-phase acetaldehyde. They found A'(~1350 cm^{-1}) = 4.5 × 10^{-18} cm molecule^{-1}, which subsequently was used by Bergner, Öberg & Rajappan (2019). However, this value has yet to be compared to an experimental result. In fact, we know of only two cases in which DFT-computed gas-phase band strengths have been compared to laboratory data for an amorphous ice. In neither case was there uniformly good agreement between theory and experiment, and perhaps none should be expected for a gas–solid comparison (Hudson 2018; Hudson & Mullikin 2019).

All of the preceding suggests a paradoxical situation in which IR reference data intended for the latest technology, such as the *James Webb Space Telescope*, are based on laboratory results from decades ago that can neither be located nor be reproduced, on measurements whose usage can be questioned, or on untested computations. To the extent that we have contributed to this confusion, we now wish to help in its clarification. In this paper we present (1) the first direct measurements of IR band intensities for amorphous acetaldehyde, $HC(O)CH_3$, (2) new IR spectra of two crystalline phases of the compound, including one for the first time, and (3) the first IR spectra and band positions for $H^{13}C(O)^{13}CH_3$. In addition, we also use the latter to make the first identification of ketene as a radiation product of solid acetaldehyde. Our new work solves the problem of questionable or untested published results for acetaldehyde being used to analyse 21st century laboratory and observational data.

2 EXPERIMENTAL METHODS

Most of the experimental details relevant to this paper have been described in previous publications from this laboratory. See particularly Hudson & Loeffler (2013) and Hudson, Loeffler & Gerakines (2017). In brief, ices were prepared by vapour-phase deposition on to a KBr substrate pre-cooled inside a vacuum chamber (~10^{-8} torr) interfaced to an IR spectrometer. Acetaldehyde, both unlabelled and labelled, was purchased from Sigma–Aldrich. It was stored at 4 °C except when in use, and was degassed by freeze-pump-thaw cycles with liquid nitrogen. No evidence was found for polymerization (Bevington & Norrish 1949). The $H^{13}C(O)^{13}CH_3$ reagent had a stated enrichment of 99 atom per cent ^{13}C. Deposition temperatures ranged from about 15 to 100 K. Laser interferometry (λ = 670 nm) was used to measure ice thicknesses, which varied from about 0.5 to 2 μm. Previous work in our laboratory gave n_{670} = 1.303 and ρ = 0.787 g cm^{-3} for the refractive index and density, respectively, of amorphous acetaldehyde near 15 K (Hudson & Coleman 2019). Deposition rates were such that the thickness of the resulting ice increased by about 1 μm in 5 min. For more on thickness measurements, see Hudson & Gerakines (2019) or Hudson & Mullikin (2019) and references therein.

IR transmission spectra were recorded with a Thermo iS50 spectrometer as 64–100 scans ratioed against the spectrum of the blank substrate, with measurements being made from 5000 to 600 cm^{-1} at a resolution of 1 cm^{-1}. Measurements also were made on a few ices, both amorphous and crystalline, at a resolution of 0.5 cm^{-1}, but the results were essentially identical to those at 1 cm^{-1} in terms of band shape, height, and width.

Sources of error and uncertainties have been discussed in previous papers from our laboratory. Two potentially large sources of error, amorphous aldehyde's density and thickness, were considerably reduced by our prior determination of both quantities. Our value of n_{670} is good to well within ±0.01 and the density error is about ±0.005 g cm^{-3}. In an earlier paper, we estimated that our uncertainties in band strengths were on the order of 5 per cent, and probably much lower, an estimate that also applies here (Hudson et al. 2017).

Our radiation experiments were with the same Van de Graaff accelerator used in our laboratory for many years (Moore & Hudson 1998), delivering 0.8 MeV protons at a beam current of about 1 × 10^{-7} A. Radiation doses were measured by a calibrated metal ring on the sample holder and were on the order of 1–20 eV molecule^{-1} which equates to about 2.4–48 MGy using a stopping power of 297.2 MeV cm^2 g^{-1} calculated with Ziegler's SRIM software with no compound correction (Ziegler 2013).

3 RESULTS

3.1 Amorphous acetaldehyde

The upper trace of Fig. 1 is a survey spectrum of an acetaldehyde ice prepared by vapour-phase deposition at 18 K. The rounded features, reminiscent of a liquid-phase spectrum, suggest that the ice was an amorphous solid, which was confirmed by spectral changes that showed crystallization on warming (see below). Table 1 gives the positions of selected peaks in the IR spectrum of the 18 K ice, rounded to the nearest 1 cm^{-1}. Many of the vibrational modes listed are considerably more complex than the simple descriptions of the table's second column. See Hollenstein & Günthard (1971) for more information.

Using the index of refraction of amorphous acetaldehyde (Hudson & Coleman 2019), we measured ice thicknesses for five ices. Standard Beer's law plots then gave the apparent absorption coefficients (α') in Table 2. Integration of the IR bands in that same table gave the apparent band strengths (A') listed, the density coming from Hudson & Coleman (2019). All correlation coeffi-

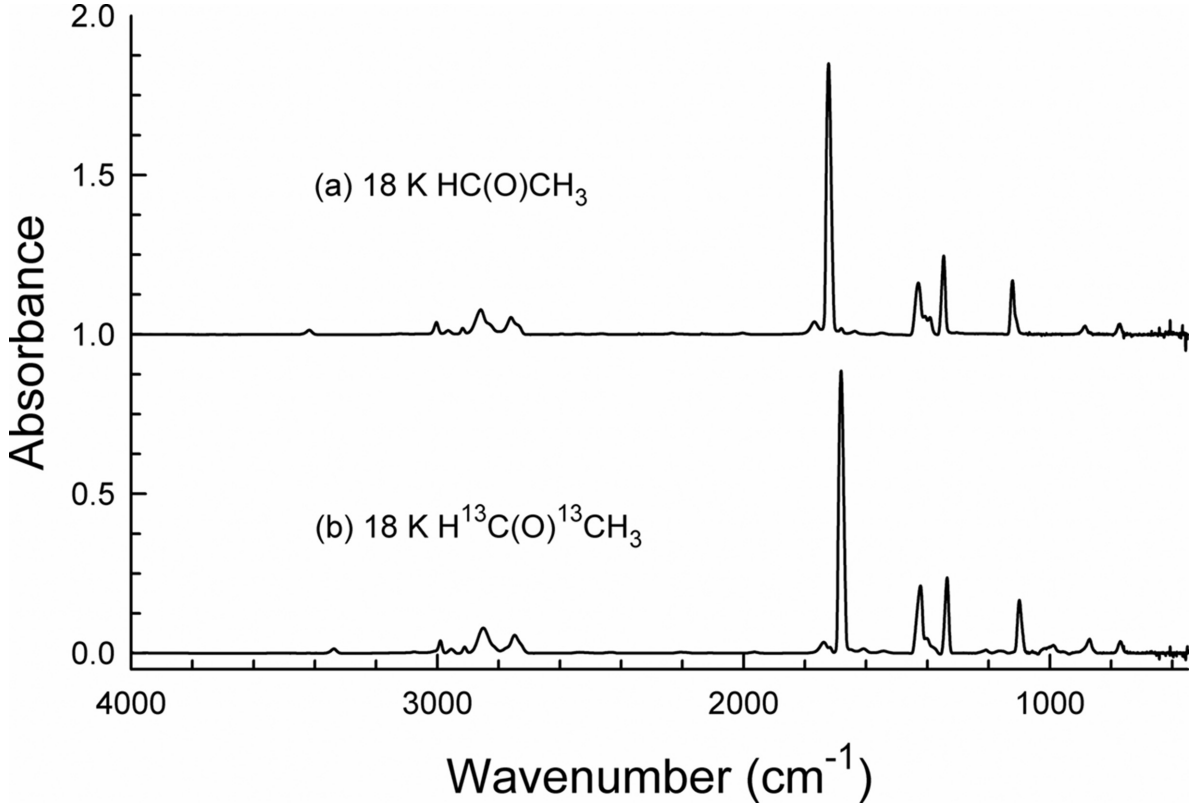

Figure 1. Survey IR spectra of amorphous acetaldehyde made and spectra recorded at 18 K. (a) $HC(O)CH_3$ and (b) $H^{13}C(O)^{13}CH_3$. Each ice's original thickness was about 1.3 μm. Spectra are offset vertically for clarity.

Table 1. Positions of selected IR features of amorphous acetaldehyde at 18 K.[a]

Vibration	Approx. description	$HC(O)CH_3$ position/cm^{-1}	$H^{13}C(O)^{13}CH_3$ position/cm^{-1}
$2\,\nu_4$	Overtone	3416	3338
ν_1	CH_3 stretch	3001	2990
ν_{11}	CH_3 stretch	2964	2954
ν_2	CH_3 stretch	2917	2911
$2\,\nu_6$	Overtone[b]	2859	2850
ν_3	CH ald. stretch	2759	2750
$2\,\nu_9$	Overtone	1768	1768
ν_4	CO stretch	1721	1682
ν_{12}	CH_3 deform	1429	1422
ν_5	CH_3 deform	–[c]	–[c]
$\nu_9 + \nu_{10}$	Combination	1409	1402
ν_6	CH bend	1391	1377
ν_7	CH_3 deform	1346	1335
ν_8	CH wag	1122	1100
ν_{13}	CH_3 deform	1102	1083
ν_9	CC rock	885	870
ν_{14}	CH_3 rock	771	769

[a]Vibrational assignments and descriptions are from Hollenstein & Günthard (1971).
[b]Positions and intensity significantly altered by Fermi resonance.
[c]Masked by other features.

Table 2. Intensities of selected IR features of amorphous acetaldehyde at 18 K.[a,b]

$HC(O)CH_3$ position/cm^{-1}	α'/cm^{-1}	Integration range/cm^{-1}	A'/cm molecule^{-1}
3416	284	3455–3375	6.28×10^{-19}
2917	331	2934–2901	3.84×10^{-19}
2858	1386	2900–2795	5.39×10^{-18}
1768	559	1810–1747	1.34×10^{-18}
1721	16970	1745–1692	2.98×10^{-17}
1428	3264	1470–1370	1.09×10^{-17}
1350	5130	1370–1320	7.11×10^{-18}
1122	3343	1150–1090	5.33×10^{-18}

[a]For each of the eight peaks listed, the absorption coefficient α' is equal to the slope of a Beer's Law graph of 2.303 × (peak height) against ice thickness. For recent examples see Hudson et al. (2017) and references therein. See also our Appendix for representative plots.
[b]For each of the eight integration ranges listed, the band strength A' is obtained from the slope of a Beer's Law graph of 2.303 × (band area) against ice thickness. In each case, the slope divided by ($\rho\, N_A$/M) gives A', where M = molar mass = 44.05 g mol^{-1}, $N_A = 6.022 \times 10^{23}$ molecules mol^{-1}, and density = 0.787 g cm^{-3}. For recent examples, see Hudson et al. (2017) and references therein. See also our Appendix for representative plots.

cients were ≥0.999 for Beer's law plots See Hudson et al. (2017) and references therein for more details and other examples of α' and A' measurements. See also our Appendix for representative plots.

Peak positions and assignments for the IR spectra of acetaldehyde have been published (e.g. Hollenstein & Günthard 1971), but we are unaware of any published spectrum for the ^{13}C isotopolog, $H^{13}C(O)^{13}CH_3$. The lower trace of Fig. 1 shows such a spectrum for an amorphous ice at 18 K, and Table 1 gives positions of selected

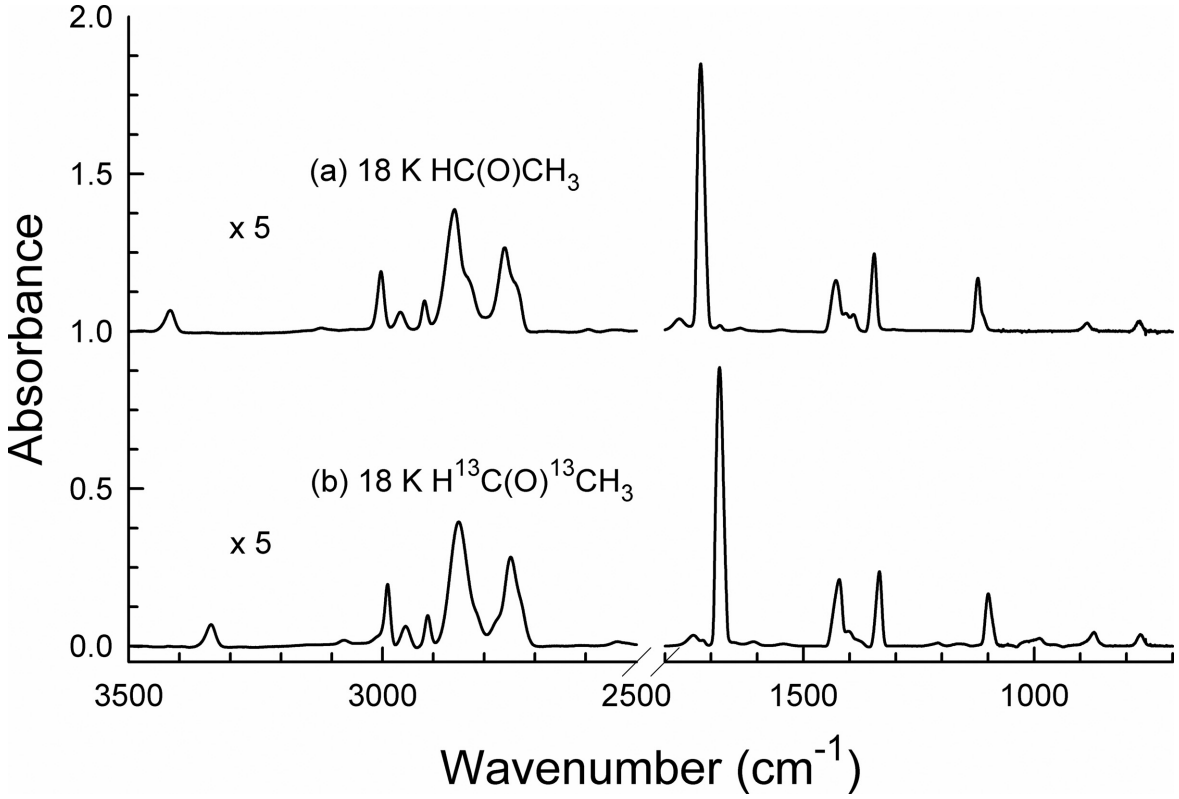

Figure 2. Expansions of several regions of the IR spectra of (a) $HC(O)CH_3$ and (b) $H^{13}C(O)^{13}CH_3$. The original thickness of each ice was about 1.3 μm. Spectra are offset vertically for clarity.

peaks. Expansions in Fig. 2 show two spectral regions for the ^{12}C and ^{13}C compounds.

The low symmetry (C_s point group) of acetaldehyde leads to a considerable number of small features due to overtones, combinations, and differences, along with peaks altered by Fermi resonance. These were largely ignored in our work because the astrochemical applications we envision will make use only of the stronger sharper features of the spectrum. One small peak we can mention is near 1680 cm^{-1} in the upper spectrum of Fig. 1. Its shift of ∼40 cm^{-1} from the carbonyl (C=O) peak suggests that the small feature is a ^{13}C satellite, and the lower spectrum of the figure confirms that assignment. A small peak near 3416 cm^{-1} in the upper spectrum is near 3338 cm^{-1} in the lower, for a ^{13}C shift of 78 cm^{-1}. This is roughly twice the ^{13}C shift of the carbonyl fundamental, as expected for an overtone vibration.

One of our group's longstanding interests is the reaction products from the low-temperature radiolysis of small molecules that either have been identified or are suspected to exist in extraterrestrial environments. Some time ago, we reported that the decomposition of amorphous ices made of either acetic acid or acetone yields ketene, H_2CCO (Hudson 2018). Therefore, it seemed reasonable to examine the radiation-induced decomposition of acetaldehyde given its structural resemblance to the other two organics, as shown in Fig. 3. Since the strongest IR band of ketene overlaps with the fundamental of CO, another expected reaction product from acetaldehyde, we carried out a radiation experiment with $H^{13}C(O)^{13}CH_3$. The IR peaks expected for ^{13}CO and $H_2{}^{13}C{}^{13}CO$, labelled ketene, are well separated. Fig. 4 shows spectra of irradiated $H^{13}C(O)^{13}CH_3$, the peak growing in at 2088 cm^{-1} being from ^{13}CO and the one rising near 2066 cm^{-1} being from $H_2{}^{13}C{}^{13}CO$. Post-irradiation warming showed that the peak for ^{13}CO decreased faster than the one for ketene, as expected. See also Hudson & Loeffler (2013) for ketene IR positions and thermal behaviour.

For the sake of completeness, we also proton-irradiated at 18 K an amorphous ice made of unlabelled $HC(O)CH_3$. After a dose of ∼1 eV $molecule^{-1}$, a peak was observed at 2129 cm^{-1}, shifting to 2136 cm^{-1} on continued irradiation. On warming to about 100 K, the peak decreased and shifted back to near 2129 cm^{-1}. We interpret this as the formation first of ketene (2129 cm^{-1}), then of CO (2136 cm^{-1}), and then the loss of CO on warming to leave ketene, consistent with Fig. 4 for $H^{13}C(O)^{13}CH_3$.

Our radiation experiments led to only a few solid-state identifications besides CO and ketene due to extensive overlap of many IR features. Relatively sharp peaks growing near 2340 and 1303 cm^{-1} were readily assigned to CO_2 and CH_4, supported by ^{13}C shifts of 65 and 8 cm^{-1}, respectively. Two small peaks rose and fell with increasing radiation dose at 1839 and 1572 cm^{-1}, each with a ^{13}C shift of about 40 cm^{-1}. The first was assigned to the acetyl radical, $CH_3\dot{C}O$, and the second to the $H_2\dot{C}C(O)H$ radical. See Hudson (2018) for a discussion and original references. Note that no peak near 1850 cm^{-1} for $H\dot{C}O$, the formyl radical, was observed. Beyond those assignments, acetaldehyde has long been known to undergo polymerization by a variety of agents, and so it is not surprising that a residue remained on our sample's KBr substrate after warming to room temperature. A polymerization mechanism based on acetaldehyde protonation has been investigated by Mansueto & Wight (1992), and seems reasonable for our radiation experiments, but detailed investigations of mechanism and products are far beyond the scope of this paper. Additional reaction products certainly can be suggested, such as ethanol, a reduction product, or diacetyl,

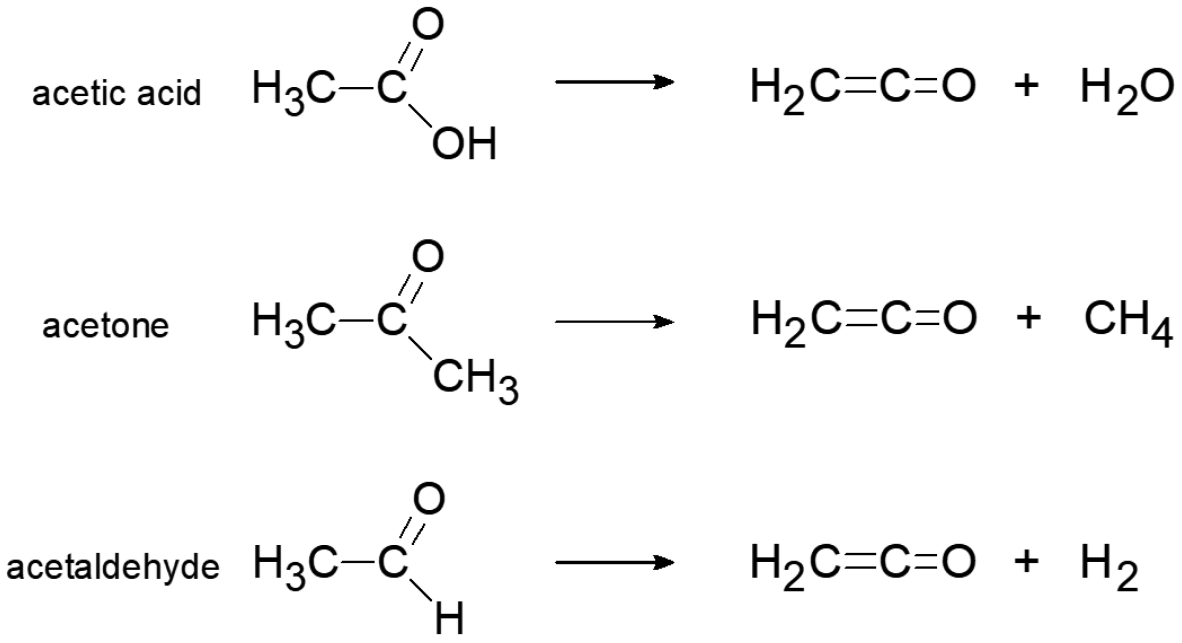

Figure 3. Some decomposition products of three organic compounds, each showing ketene.

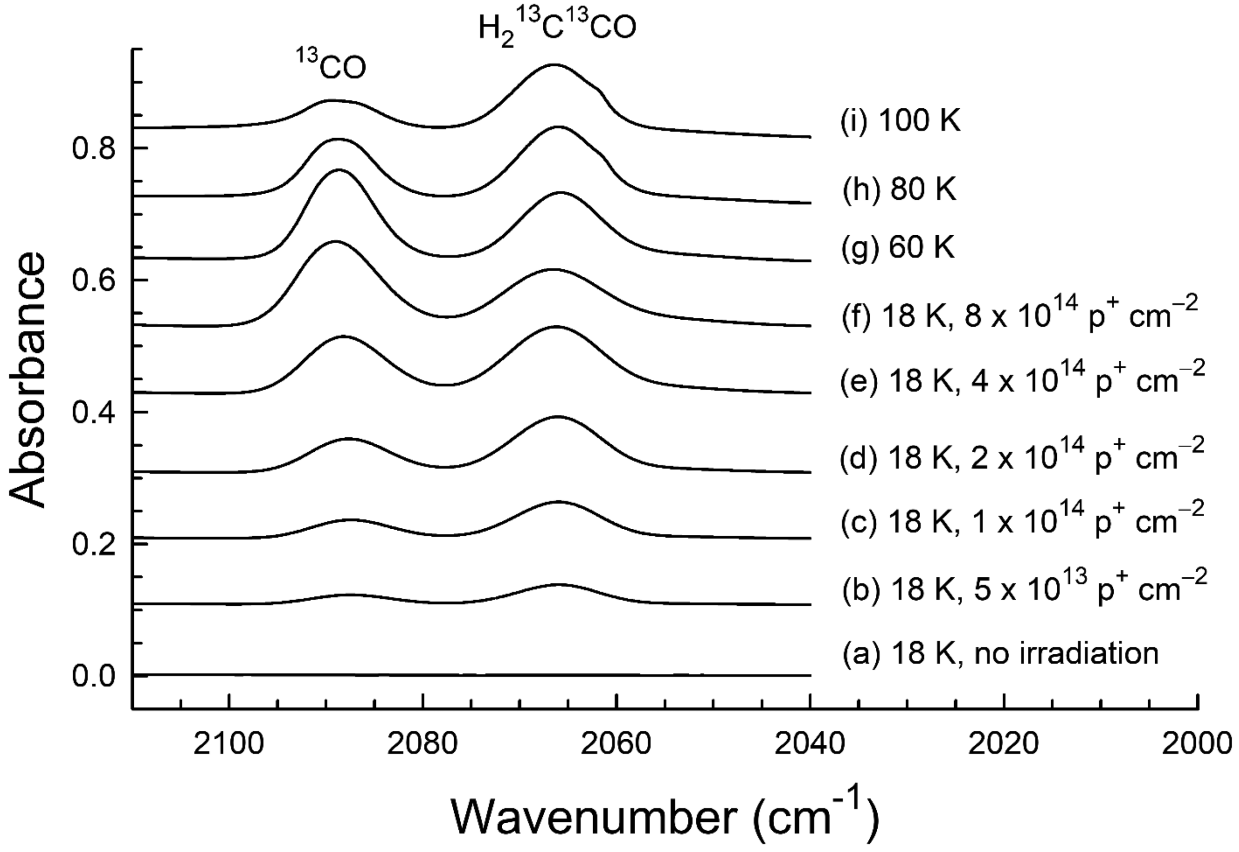

Figure 4. From bottom to top, the irradiation of amorphous $H^{13}C(O)^{13}CH_3$ at 18 K, showing the formation of an IR feature near 2088 cm^{-1} for ^{13}CO and 2066 cm^{-1} for $H_2{}^{13}C{}^{13}CO$ (ketene), and then the decrease in ^{13}CO on warming to 100 K. Spectra are offset for clarity. A fluence of 1×10^{14} p^+ cm^{-2} is equivalent to a dose of about 2 eV $molecule^{-1}$.

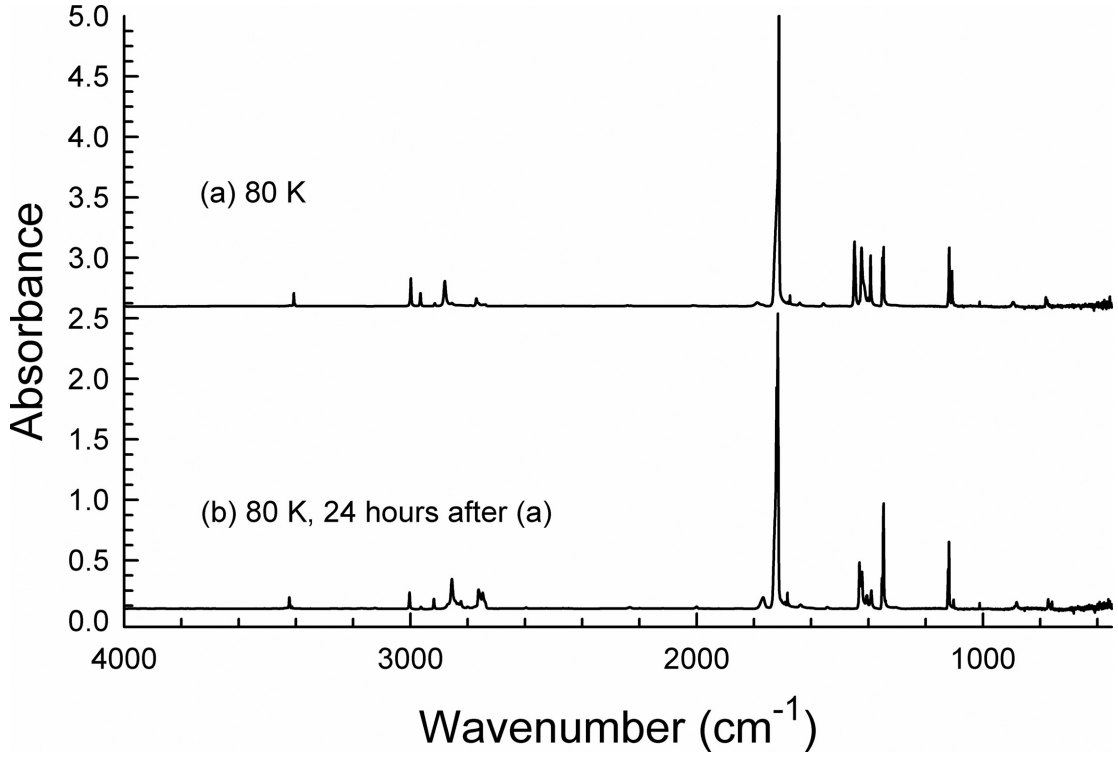

Figure 5. Survey spectra of crystalline acetaldehyde. (a) The spectrum of an ice made by vapour-phase deposition at 80 K. (b) The spectrum of the same ice at 80 K after being held at 80 K for 24 h. The ice's original thickness was about 1.3 μm. Spectrum (b) also was obtained on deposition of an ice at 100 K or on warming from 80 to 100 K over a few minutes. It is the crystalline acetaldehyde spectrum found in the literature (e.g. Hollenstein & Günthard 1971).

$(CH_3CO)_2$, from radical dimerization, but the complexity of our IR spectra make all such suggestions highly speculative.

3.2 Crystalline acetaldehyde

Although our focus was mainly on the amorphous form of acetaldehyde, because of its possible astrochemical applications, several observations related to crystalline acetaldehyde are of interest. Before beginning our work, we knew from the neutron-diffraction study of Ibberson, Yamamuro & Matsuo (2000) that it should be possible to make two crystalline forms of acetaldehyde under our conditions. One of the two forms was easy to prepare, being obtained either by heating amorphous acetaldehyde to 75–80 K or by vapour-phase deposition at 100 K and higher. The spectrum recorded agreed with the literature spectrum of, and the peaks listed by, Hollenstein & Günthard (1971). We could not record IR spectra above about 120 K due to rapid sublimation of the acetaldehyde ices in our vacuum system.

The second crystalline polymorph was more difficult to prepare. By vapour depositing acetaldehyde at 80 K we obtained a spectrum that was not found in the literature. See the upper trace of Fig. 5. Holding that same ice at 80 K for 24 h gave the lower spectrum of Fig. 5, the aforementioned spectrum of the crystalline solid. Figs 6 and 7 show expansions of four regions over that same 24-h period, and illustrate the smooth conversion from one crystalline form to the other. Isosbestic points near 3001, 2871, 1436, 1427, 1408, 1402, and 1119 cm^{-1} were consistent with an interpretation of there being no intermediate phase. These same changes were observed in only a few minutes when an ice grown at 80 K was warmed to 100 K. Note that the spectrum of (b) in Fig. 5 was never seen to convert into the spectrum of (a). Band strengths and absorption coefficients were not calculated for these crystalline ices, but positions of selected peaks are listed in Table 3. Changes similar to those just described were obtained with $H^{13}C(O)^{13}CH_3$, but a lack of material prohibited an extensive study. Table 4 gives peak positions of the two crystalline phases of $H^{13}C(O)^{13}CH_3$, isotopic data we have not found in the literature for either crystalline form.

4 DISCUSSION

4.1 IR spectral positions and intensities

It is difficult to locate IR spectra of ices for comparison to our own, but we note that Terwisscha van Scheltinga et al. (2018) published a spectrum of amorphous acetaldehyde at 15 K and Ioppolo et al. (2014) published one of crystalline acetaldehyde at 125 K. Those two published spectra closely resemble ours, and the few peak positions given in each case agree with the results in our tables. The paper of Terwisscha van Scheltinga et al. (2018) has four acetaldehyde relative band strengths, and they too are close to ours. As an example, the ratio of intensities of the strong 1721 cm^{-1} band in amorphous acetaldehyde to the 1350 cm^{-1} band is 4.3 in their work and 4.2 in our own.

As for absolute band strengths, in our Introduction we noted problems with all three values in use. The only IR feature common to the earlier studies is the one at 1350 cm^{-1} for amorphous acetaldehyde. Compared to the direct measurement reported here, the per cent errors in A'(1350 cm^{-1}) are 14 per cent (Moore & Hudson 1998), 37 per cent (Bennett et al. 2005), and 79 per cent (Schutte et al. 1999). However, given the concerns about each of these three earlier determinations of A', it is difficult to decide whether any agreement or disagreement is not simply fortuitous. Band strengths also have

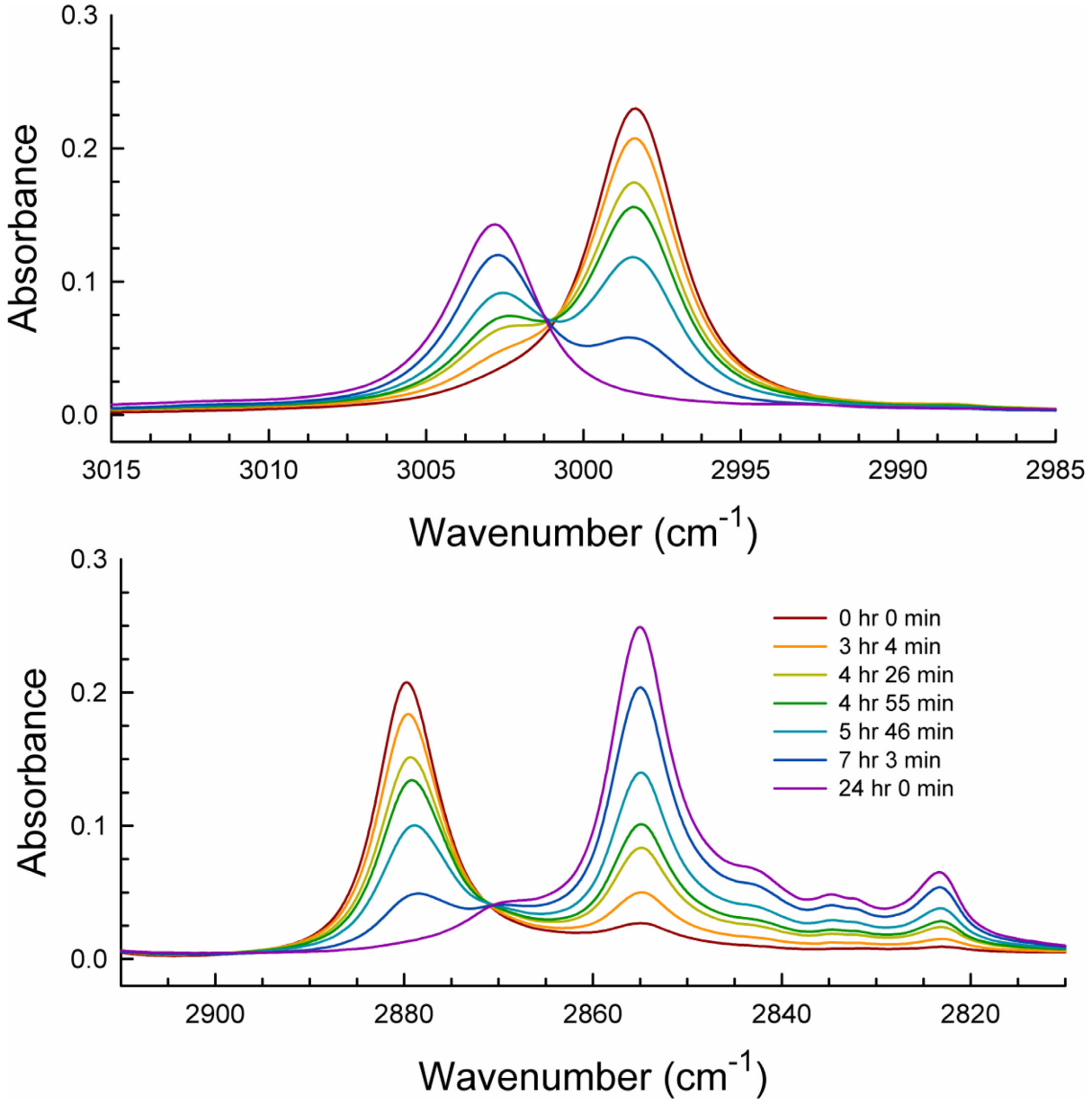

Figure 6. Expansions of IR spectra of acetaldehyde showing the conversion from the metastable form to the stable crystalline phase at 80 K over 24 h. The ice's original thickness was about 1.3 μm, and the ice was made by deposition at 80 K. Peaks near 2998 and 2880 cm^{-1} are decreasing while peaks near 3003 and 2855 cm^{-1} are increasing. The spectra shown were recorded at the times indicated.

been reported for gas-phase acetaldehyde, but again are difficult to interpret and compare to what has been presented here. For example, limits of integration were not stated by either Rogers (1985) or Wiberg et al. (1995) and it is not known if any curve-fitting routines were used to deconvolve complex features.

Another way to evaluate our results is to select one IR feature that acetaldehyde possesses in common with molecules already studied, an obvious candidate being the carbonyl stretching vibration. For the C=O stretch of amorphous acetaldehyde, we measured a band strength of 2.98×10^{-17} cm molecule^{-1}, compared to 4.96 and 2.67×10^{-17} cm molecule^{-1} for amorphous methyl formate and acetone, respectively (Modica & Palumbo 2010; Hudson & Mullikin 2019). Our result seems reasonable when compared to those two values.

Turning from the spectra of amorphous acetaldehyde to those of the crystalline forms, our Fig. 5 shows two distinct IR spectra and two polymorphs have been reported (Ibberson et al. 2000). The spectrum at the bottom of the figure was never seen to convert into the one at the top, and so the lower spectrum is assigned to the stable form of crystalline acetaldehyde at 15–120 K, the temperature range of our experiments. In contrast, the upper spectrum of that same figure was seen to smoothly convert into the lower spectrum, as seen in Figs 6 and 7. Therefore, we assign that upper spectrum, prepared by deposition of an ice at 80 K, to the metastable form of crystalline acetaldehyde reported by Ibberson et al. (2000). The stable form appears to be the same as that of Hollenstein & Günthard (1971), based on the close agreement between the peak positions they reported and the values in our Table 3.

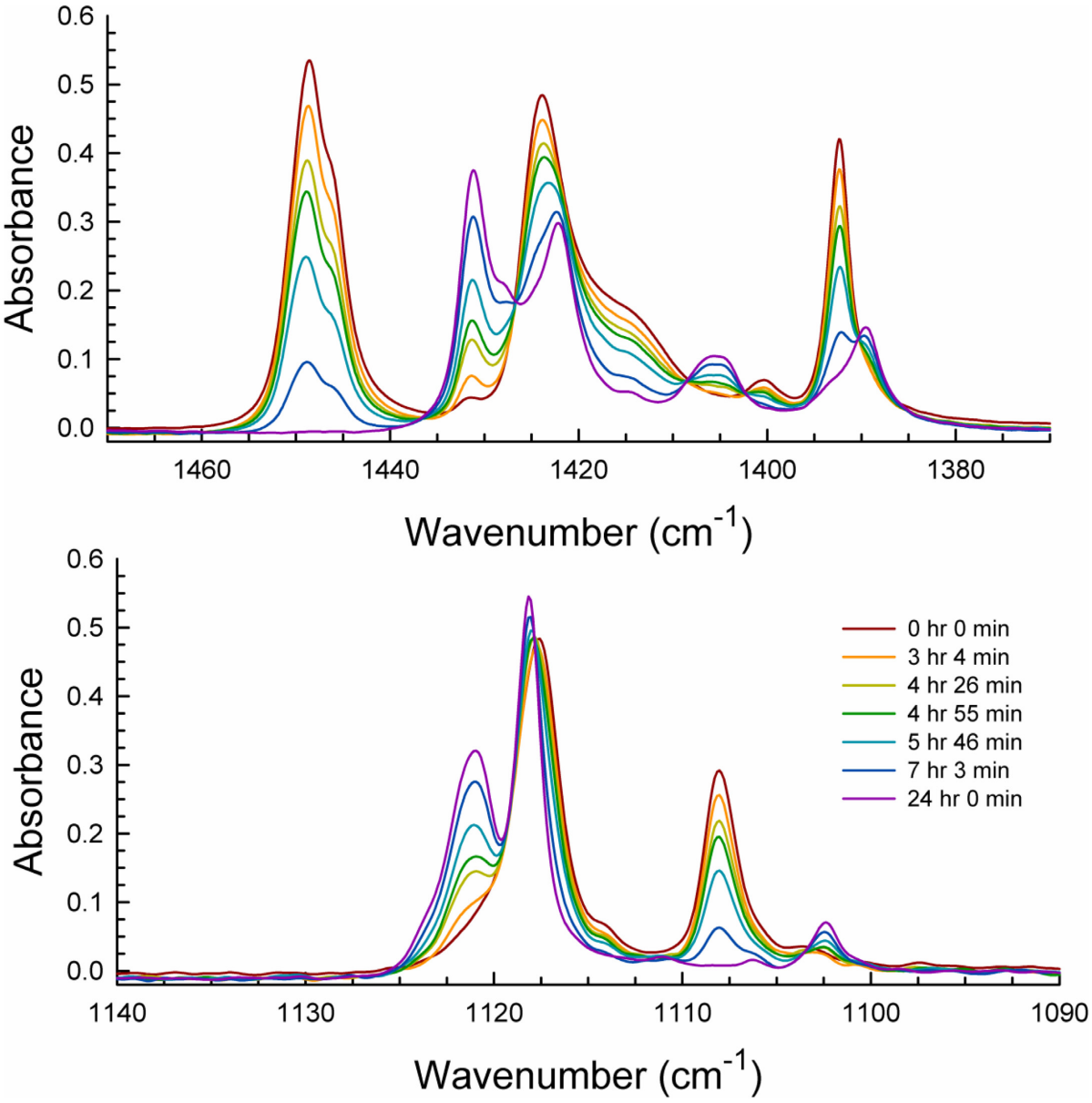

Figure 7. Expansions of IR spectra of acetaldehyde showing the conversion from the metastable form to the stable crystalline phase at 80 K over 24 hours. The ice's original thickness was about 1.3 μm, and the ice was made by deposition at 80 K. Peaks near 1449, 1424, 1392, and 1108 cm^{-1} are decreasing while peaks near 1431, 1407, and 1118 cm^{-1} are increasing. The spectra shown were recorded at the times indicated.

It is interesting that warming amorphous acetaldehyde from 18 to 80 K produces the *high*-temperature stable crystalline polymorph and not the metastable solid. Responsibility for this behaviour may reside with the Ostwald Step Rule, which states that the solid that forms first on crystallization is the kinetically favoured one, as opposed to the thermodynamically most stable solid. We suspect that formation of the metastable ice phase requires a combination of the heat of condensation released at 80 K and the added molecular mobility at 80 K compared to 18 K, so that simply warming from 18 to 80 K is insufficient to make what we termed the metastable form. An illustration and discussion of similar behaviour is found in the work of Tizek, Grothe & Knözinger (2004) in a careful X-ray diffraction study of the two crystalline forms of acetonitrile, CH_3CN. For another example, see our study of the two crystalline forms of CH_3SH (Hudson 2016).

4.2 Radiation experiment

The question we sought to answer with our radiation experiment was whether ketene is a radiolysis product of solid acetaldehyde, and our results leave no doubt that it is. Over a century ago, Wilsmore & Stewart (1907) suggested that molecules with the structural unit $-CH_2-C(=O)-X$ would decompose to give ketene ($H_2C=C=O$) as a product. Those authors' work did not include solid-phase results, but their suggestion has now been confirmed by us for solid acetone, acetic acid, and acetaldehyde (Fig. 3). See Hudson (2018) and references therein for additional details and chemical reactions. It would be interesting to conduct matrix-isolation radiation experiments with acetaldehyde trapped in a rare-gas solid to see if pairs of reaction products (e.g. CO + CH_4 or H_2 + ketene) could be detected in the same matrix site. We encourage the use of isotopically enriched reagents for such work

Table 3. Positions of selected IR features of crystalline acetaldehyde.[a]

Vibration	Approx. description	$HC(O)CH_3$ position/cm^{-1} Stable phase	$HC(O)CH_3$ position/cm^{-1} Metastable phase	$HC(O)CH_3$ position/cm^{-1} Literature[a]
$2\,\nu_4$	Overtone	3423	3407	3422
ν_1	CH_3 stretch	3003	2998	3003
ν_{11}	CH_3 stretch	2964	2965	2964
ν_2	CH_3 stretch	2918	2915	2918
$2\,\nu_6$	Overtone[b]	2855	2880	2855
ν_3	CH ald. stretch	2762, 2747	2770, 2762	2762, 2747
$2\,\nu_9$	Overtone	1768	1787, 1769	1768
ν_4	CO stretch	1721, 1717	1713	1722, 1716
ν_{12}	CH_3 deform	1431	1449	1431
ν_5	CH_3 deform	1422	1424	1422
$\nu_9 + \nu_{10}$	Combination	1407	1414?	1406
ν_6	CH bend	1393, 1389	1392	1392, 1389
ν_7	CH_3 deform	1353, 1348	1351, 1347	1352, 1347
ν_8	CH wag	1121, 1119	1118, 1108	1120, 1118
ν_{13}	CH_3 deform	1102	1103	1102
ν_9	CC rock	889, 883, 875	894, 883	889, 882, 875
ν_{14}	CH_3 rock	772, 770	780, 775	772, 770, 766

[a]Vibrational assignments, descriptions, and literature positions are from Hollenstein & Günthard (1971), and their sample's temperature was 77 K. The data from the present work are for 80 K ices.
[b]Positions and intensity significantly altered by Fermi resonance.

Table 4. Positions of selected IR features of crystalline acetaldehyde-$^{13}C_2$.[a]

Vibration	Approx. description	$H^{13}C(O)^{13}CH_3$ position/cm^{-1} Stable phase	$H^{13}C(O)^{13}CH_3$ position/cm^{-1} Metastable phase
$2\,\nu_4$	Overtone	3344	3329
ν_1	CH_3 stretch	2992	2987
ν_{11}	CH_3 stretch	2954	2955
ν_2	CH_3 stretch	2913	2912, 2909
$2\,\nu_6$	Overtone[b]	2847	2870
ν_3	CH ald. stretch	2749, 2734	2758, 2748
$2\,\nu_9$	Overtone	1738	1756, 1739
ν_4	CO stretch	1683, 1678	1674
ν_{12}	CH_3 deform	1427	1444
ν_5	CH_3 deform	1418	1420
$\nu_9 + \nu_{10}$	Combination	1402	1408?
ν_6	CH bend	1374	1382
ν_7	CH_3 deform	1342, 1337	1349, 1346
ν_8	CH wag	1098, 1096	1096, 1088
ν_{13}	CH_3 deform	1083	1084?
ν_9	CC rock	875, 868	879, 868
ν_{14}	CH_3 rock	769, 767	777, 772

[a]Vibrational assignments and descriptions are from Hollenstein & Günthard (1971). The data from the present work are for 80 K ices.
[b]Positions and intensity significantly altered by Fermi resonance.

as the ketene we observed was not reported by Della Védova & Sala (1991) in experiments involving the photolysis of natural-abundance acetaldehyde in solid Ar or N_2. It is not known if the non-observation was related to the experimental conditions or a lack of ketene formation.

As already mentioned, in our experiments only a few radiation products were identified due to the extensive overlap of IR features. Among the products found were the $CH_3\dot{C}O$ and $H_2\dot{C}C(O)H$ radicals. These might be dissociation products of excited acetaldehyde, formed by C—H bond dissociation, but since acetaldehyde's C—C bond is weaker than either of its C—H bonds (da Silva & Bozzelli 2006) one might also expect to observe the $H\dot{C}O$ radical (formyl radical) as a product, which we never saw. One explanation for the non-observation of $H\dot{C}O$ can be found by considering the initial events of the radiolysis through the reactions below.

$$HC(O)CH_3 \rightarrow [HC(O)CH_3]^{\bullet+} + e^- \quad (1)$$

$$[HC(O)CH_3]^{\bullet+} + HC(O)CH_3 \rightarrow \dot{C}(O)CH_3 + [HC(OH)CH_3]^+ \quad (2)$$

$$[HC(O)CH_3]^{\bullet+} + HC(O)CH_3 \rightarrow HC(O)\dot{C}H_2 + [HC(OH)CH_3]^+ \quad (3)$$

The radical cation formed in reaction (1) can either abstract a hydrogen atom from a neighbouring acetaldehyde molecule or it can act as an acid and transfer H^+ to another acetaldehyde molecule. In either case, the resulting two products are the same, as seen in reactions (2) and (3). Since there are only two sites in acetaldehyde for either H-atom abstraction or H^+ transfer then only two radical products should result, the two shown in reactions (2) and (3), and those are the two radicals we observed in our IR spectra. A different possibility for the non-observance of $H\dot{C}O$ is that it is formed by dissociation of excited $HC(O)CH_3$ followed by rapid disproportionation of the resulting $H\dot{C}O$ and $\dot{C}H_3$ radicals to give the molecular products CO and CH_4 observed.

4.3 Astrochemical applications

The expected low abundance of most organics in interstellar and cometary ices, and on the surface of an icy satellite, suggests that the use of our new spectra and intensity data for a direct IR observation of solid acetaldehyde is of low probability. More likely is that the work reported here will be used in laboratory investigations of reactions known or expected to occur in icy extraterrestrial environments. Our results will aid in the preparation of multicomponent ices containing acetaldehyde by allowing for calibrations and determinations of that compound in an ice sample. We also envision applications of our data to the measurement of reaction yields in experiments that might produce acetaldehyde in polar ices. Our IR intensities also can be used to estimate band strengths in spectral regions beyond the mid-IR used in the present work. See Gerakines et al. (2005) for an example.

Astrochemical results based on IR band strengths published before those presented here can now be updated with our new measurements. For example, and as already described, the reference band strength of Schutte et al. (1999) for amorphous acetaldehyde's CH_3 deformation at 1350 cm^{-1} is $A' = 1.5 \times 10^{-18}$ cm molecule^{-1}, which now is seen to be in error by nearly 80 per cent. Molecular abundances or column densities based on that older A' will be in error by that much, although published relative band strengths might not change substantially.

Finally, we again point out that few aldehydes have been examined with the methods used here. As an example, propionaldehyde (propanal) is an interstellar molecule, and at least two laboratory papers recently have been published involving it (Jonusas, Guillemin & Krim 2017; Qasim et al. 2019), but no band strength measurements are available for the solid compound. The situation is no better for H_2CO (formaldehyde). Many laboratory papers have been published involving H_2CO, but only estimates and indirect measurements are available for its IR intensities. Unfortunately, their accuracy is unknown.

5 SUMMARY AND CONCLUSIONS

Here we have reported the first direct measurements of band intensities of solid acetaldehyde, removing the need to rely on either calculated gas-phase results or values that cannot be traced to their original source. We also have presented mid-IR spectra of the two crystalline polymorphs previously identified by neutron-diffraction studies, one stable under our conditions and one metastable. The IR spectrum of $H^{13}C(O)^{13}CH_3$ has been recorded and used to identify ketene as a radiolytic decomposition product of solid acetaldehyde for the first time.

ACKNOWLEDGEMENTS

We acknowledge the support of NASA's Planetary Science Division Internal Scientist Funding Program through the Fundamental Laboratory Research (FLaRe) work package at the NASA Goddard Space Flight Center. That funding allowed for a substantial, significant upgrade of the equipment used for this work. We also acknowledge the financial support of the NASA Astrobiology Institute through funding awarded to the Goddard Center for Astrobiology under proposal 13-13NAI7-0032. Richard Ibberson of Oak Ridge National Laboratory is thanked for correspondence about his neutron diffraction work.

REFERENCES

Bennett C. J., Jamieson C. S., Osamura Y., Kaiser R. I., 2005, ApJ, 624, 1097
Bergner J. B., Öberg K. I., Rajappan M., 2019, ApJ, 874, 115
Bevington J. C, Norrish R. G. W., 1949, Proc. R. Soc. A, 196, 363
Crovisier J., Bockelée-Morvan D., Colom P., Biver N., Despois D., Lis D. C., and the team for target-of-opportunity radio observations of comets, 2004, A&A, 418, 1141
Dartois E., 2005, Space Sci. Rev., 119, 293
da Silva G., Bozzelli J. W., 2006, J. Phys. Chem. A, 110, 13058
Della Védova C. O., Sala O., 1991, J. Raman Spectrosc., 22, 505
Enrique-Romero J., Rimola A., Ceccarelli C., Balucani N., MNRAS, 2016, 459, L6
Enrique-Romero J., Rimola A., Ceccarelli C., Ugliengo P., Balucani N., Skouteris D., , 2019, ACS Earth Space Sci., 3, 2158
Fourikis N., Sinclair M. W., Robinson B. J., Godfrey P. D., Brown R. D., 1974, Aust. J. Phys., 27, 425
Fresneau A., Danger G., Rimola A., Duvernay F., Theulé P., Chiavassa T., 2015, MNRAS, 451, 1649
Gerakines P. A., Hudson R. L., 2015, ApJ, 805, L20
Gerakines P. A., Bray J. J., Davis A., Richey C. R., 2005, ApJ, 620, 1140
Gibb E. L., Whittet D. C. B., Boogert A. C. A., Tielens A. G. G. M., 2004, ApJS, 151, 35
Hollenberg J. L., Dows D. A., 1961, J. Chem. Phys., 34, 1061
Hollenstein H., Günthard Hs. H., 1971, Spectrochim. Acta, 27A, 2027
Hollis J. M., Jewell P. R., Lovas F. J., Remijan A., Møllendal H., 2004, ApJ, 610, L21
Hudson R. L., 2016, Phys. Chem. Chem. Phys., 18, 25756
Hudson R. L., 2018, Phys. Chem. Chem. Phys., 20, 5389
Hudson R. L., Coleman F. M., 2019, Phys. Chem. Chem. Phys., 21, 11284
Hudson R. L., Gerakines P. A., 2019, MNRAS, 482, 4009
Hudson R. L., Loeffler M. J., 2013, ApJ, 773, 773
Hudson R. L., Mullikin E. F., 2019, Spectrochim. Acta, 207, 216
Hudson R. L., Gerakines P. A., Moore M. H., 2014, Icarus, 243, 148
Hudson R. L., Loeffler M. J., Gerakines P. A., 2017, J. Chem. Phys., 146, 0243304
Ibberson R. M., Yamamuro O., Matsuo T., 2000, J. Molec. Struct., 520, 265
Ioppolo S., McGuire B. A., Allodi M. A., Blake G. A., 2014, Faraday Discuss, 168, 461
Jonusas M., Guillemin J.-C., Krim L., 2017, MNRAS, 468, 4592
Maeda S., Schatz P. N., 1961, J. Chem. Phys., 35, 1617
Mansueto E. S., Wight C. A., 1992, J. Phys. Chem., 96, 1502
Modica P., Palumbo M. E., 2010, A&A, 519, A22
Moore M. H., Hudson R. L., 1998, Icarus, 135, 518
Öberg K. I., Garrod R. T., van Dishoeck E. F., Linnartz H., 2009, A&A, 504, 891
Öberg K. I., van Dishoeck E. F., Linnartz H., Andersson S., 2010, ApJ, 718, 832
Qasim D. et al., 2019, A&A, 627, A1
Rogers J. D., 1985, J. Quant. Spectr. Radiat. Trans., 34, 27
Schutte W. A. et al., 1999, A&A, 343, 966
Snyder L. E., Buhl D., Zuckerman B., Palmer P., Phys. Rev. Lett., 1969, 22, 679
Terwisscha van Scheltinga J., Ligterink N. F. W., Boogert A. C. A., van Dishoeck E. F., Linnartz H., 2018, A&A, 611, A35
Tizek H., Grothe H., Knözinger E., 2004, Chem. Phys. Lett., 383, 129
Vinogradoff V., Duvernay F., Farabet M., Danger G., Theule´ P., Borget F., Guillemin J. C., Chiavassa T., 2012, J. Phys. Chem., 116, 2225
Wexler A. S., 1967, Appl. Spec. Rev., 1, 29
Wiberg K. B., Thiel Y., Goodman L., Leszczynski J., 1995, J. Phys. Chem., 99, 13850
Wilsmore N. T. M., Stewart A. W., 1907, Nature, 75, 510
Ziegler J. F., 2013, Stopping and range of ions in matter SRIM2008(www.srim.org)

APPENDIX A

The procedure used to determine absorption coefficients (α') and band strengths (A') is the same as in our earlier papers, and is essentially the method of Hollenberg & Dows (1961). Briefly, IR spectra were recorded of ice samples having a range of thicknesses. The absorbance at each peak of interest was measured and bands of interest were integrated. Multiplication of each absorbance or band area by $\ln(10) \approx 2.303$ was then done to convert from a common to a natural logarithmic scale. Representative plots of the results are shown in Fig. A1. The slope of the upper graph is α' and the slope of the lower one is $(A'\rho N_A/M)$, where M = molar mass = 44.05 g mol^{-1}, $N_A = 6.022 \times 10^{23}$ molecules mol^{-1}, and density (ρ) = 0.787 g cm^{-3}. From this slope A' is calculated. For recent examples, see Hudson, Gerakines & Moore (2014), Gerakines & Hudson (2015), Hudson et al. (2017), and references therein to even older papers by our group and others.

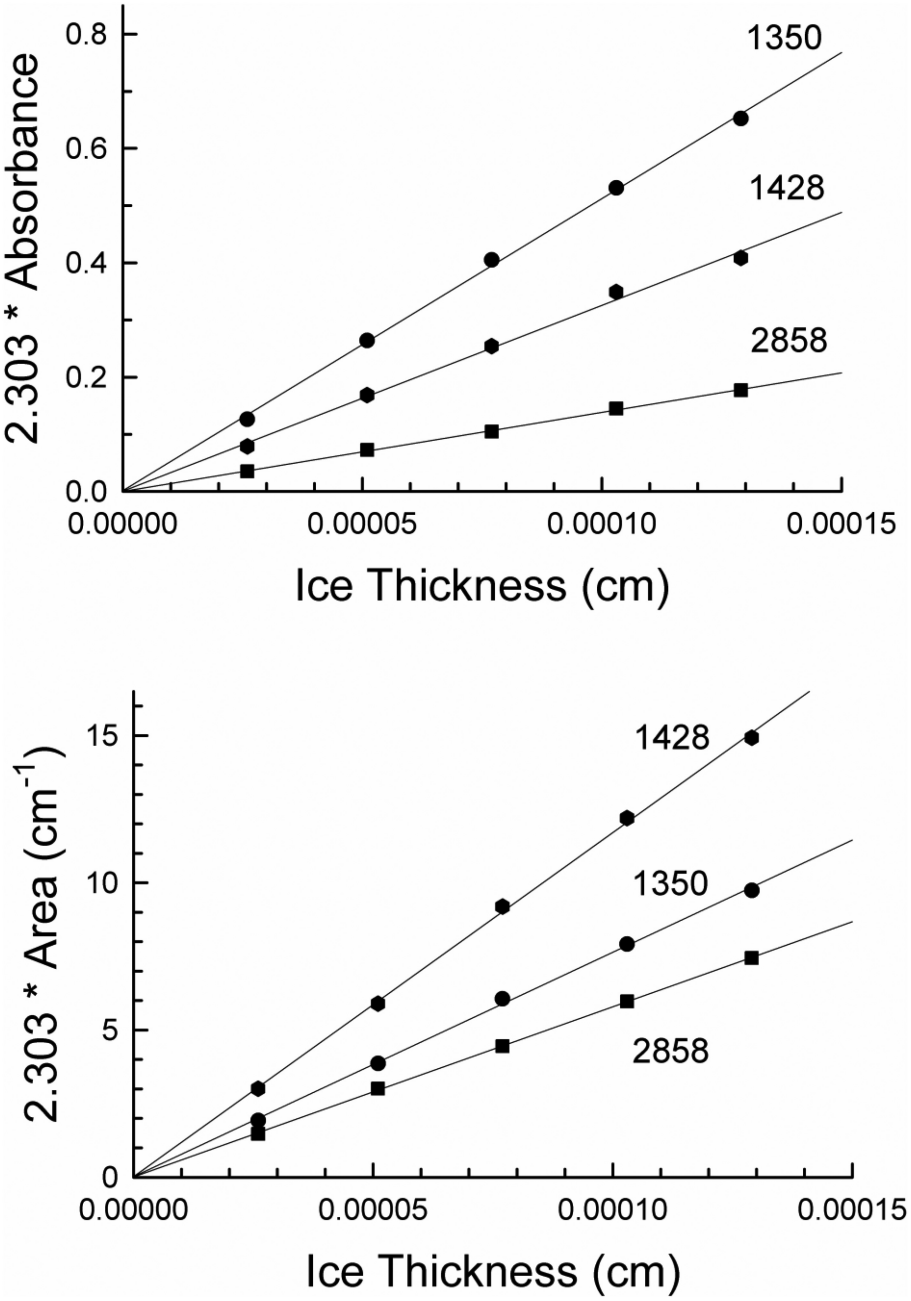

Figure A1. Representative Beer's Law plots for the determination of absorption coefficients (α') and band strengths (A'). Approximate positions, in cm^{-1}, of three IR features are indicated.

This paper has been typeset from a Microsoft Word file prepared by the author.